Planta (2012) 236:1419–1431
DOI 10.1007/s00425-012-1694-y

ORIGINAL ARTICLE

Deciphering the route of *Ralstonia solanacearum* colonization in *Arabidopsis thaliana* roots during a compatible interaction: focus at the plant cell wall

Catherine Digonnet · Yves Martinez · Nicolas Denancé · Marine Chasseray · Patrick Dabos · Philippe Ranocha · Yves Marco · Alain Jauneau · Deborah Goffner

Received: 22 May 2012 / Accepted: 11 June 2012 / Published online: 24 June 2012

Abstract The compatible interaction between the model plant, *Arabidopsis thaliana*, and the GMI1000 strain of the phytopathogenic bacterium, *Ralstonia solanacearum*, was investigated in an in vitro pathosystem. We describe the progression of the bacteria in the root from penetration at the root surface to the xylem vessels and the cell type-specific, cell wall-associated modifications that accompanies bacterial colonization. Within 6 days post inoculation, *R. solanacearum* provoked a rapid plasmolysis of the epidermal, cortical, and endodermal cells, including those not directly in contact with the bacteria. Plasmolysis was accompanied by a global degradation of pectic homogalacturonanes as shown by the loss of JIM7 and JIM5 antibody signal in the cell wall of these cell types. As indicated by immunolabeling with Rsol-I antibodies that specifically recognize *R. solanacearum*, the bacteria progresses through the root in a highly directed, centripetal manner to the xylem poles, without extensive multiplication in the intercellular spaces along its path. Entry into the vascular cylinder was facilitated by cell collapse of the two pericycle cells located at the xylem poles. Once the bacteria reached the xylem vessels, they multiplied abundantly and moved from vessel to vessel by digesting the pit membrane between adjacent vessels. The degradation of the secondary walls of xylem vessels was not a prerequisite for vessel colonization as LM10 antibodies strongly labeled xylem cell walls, even at very late stages in disease development. Finally, the capacity of *R. solanacearum* to specifically degrade certain cell wall components and not others could be correlated with the arsenal of cell wall hydrolytic enzymes identified in the bacterial genome.

Keywords *Arabidopsis* · Cell wall · Cytology · Plant–pathogen interaction · *Ralstonia* · Root

Abbreviations

dpi	Days post-inoculation
HG	Homogalacturonan
PEL	Pectate lyase
PG	Polygalacturonase
PL	Pectin lyase

C. Digonnet and Y. Martinez contributed equally to this work.

Electronic supplementary material The online version of this article (doi:10.1007/s00425-012-1694-y) contains supplementary material, which is available to authorized users.

C. Digonnet · N. Denancé · M. Chasseray · P. Ranocha · D. Goffner (✉)
Université de Toulouse, UPS, UMR 5546, Laboratoire de Recherche en Sciences Végétales, BP 42617, 31326 Castanet-Tolosan, France
e-mail: goffner@lrsv.ups-tlse.fr

C. Digonnet · N. Denancé · M. Chasseray · P. Ranocha · D. Goffner
Centre National de la Recherche Scientifique, CNRS, UMR 5546, Laboratoire de Recherche en Sciences Végétales, BP 42617, 31326 Castanet-Tolosan, France

Y. Martinez · A. Jauneau
Centre National de la Recherche Scientifique, CNRS, Plateforme Imagerie-Microscopie, Fédération de Recherche FR3450, 24 Chemin de Borde Rouge, 31326 Castanet-Tolosan, France

P. Dabos · Y. Marco
Institut National de la Recherche Agronomique, INRA, UMR 441, Laboratoire des Interactions Plantes Microorganismes, 24 Chemin de Borde Rouge, 31326 Castanet-Tolosan, France

P. Dabos · Y. Marco
Centre National de la Recherche Scientifique, CNRS, UMR 2594, Laboratoire des Interactions Plantes Microorganismes, 24 Chemin de Borde Rouge, 31326 Castanet-Tolosan, France

PME Pectin methylesterase
TEM Transmission electron microscopy

Introduction

A plant cell wall surrounds each individual plant cell. It is a complex structure composed of cellulose, hemicelluloses, pectin, and proteins and undergoes compositional and structural changes during the course of normal plant development or in response to abiotic and biotic stress (for review, see Cosgrove 2005; Scheller and Ulvskov 2010; Carpita 2011). However, there is certain degree of heterogeneity of wall components, either at the species, organ, and even cellular levels (Burton et al. 2010). To study this diversity, nearly 200 monoclonal antibodies have been developed that recognize specific wall epitopes, largely facilitating the study of the structure, dynamic events and biosynthesis of plant cell walls at the cellular level (Pattathil et al. 2010).

Due to its strategic localization at the plant–environment interface, it is reasonable to assume that cell walls contribute to the outcome of plant–pathogen interactions and there is increasing genetic evidence underlining the importance of the cell wall in plant defense (Huckelhoven 2007). Indeed, several primary cell wall Arabidopsis mutants that develop resistance to *Agrobacterium tumefaciens* (*rat*) or powdery mildew pathogens (*pmr*) have been identified (Vogel and Somerville 2000; Vogel et al. 2002, 2004; Zhu et al. 2003a, b). Similarly, mutations in two different subunits of the cellulose synthase complex (CESA) that are specific for cellulose synthesis in the secondary wall led to full resistance to *Ralstonia solanacearum* and the fungus, *Plectosphaerella cucumerina*, in *irx1-6[irregular xylem1-6]/cesa8* and *irx5-5/cesa4* mutants (Hernandez-Blanco et al. 2007).

The success of a given pathogen also depends on its capacity to degrade plant cell walls as it progresses within the host. Many pathogens possess enzymatic arsenals allowing the degradation of pectin including pectin methylesterases (PME), pectin lyases (PL), pectate lyases (PEL), and polygalacturonases (PG) and their enzyme efficiency is in some cases necessary for full virulence. For example, loss of function of *Botrytis cinerea BcPME1* results in the reduction of apple maceration during infection (Valette-Collet et al. 2003), whereas virulence of *Claviceps purpura* on rye is nearly abolished in a strain mutated in two polygalacturonases genes, *CpPG1* and *CpPG2* (Oeser et al. 2002). The bacterium, *Xanthomonas campestris* pv. *campestris* (*Xcc*), also possesses cell wall-degrading enzymes and interestingly, two genes coding a PME and a PEL are located close to the TBDT (TonB-dependent transporter) *XCC0120* gene, suggesting the existence of a CUT system (Carbohydrate Utilization containing TBDT locus) required for pectin degradation by the bacterium (Blanvillain et al. 2007).

The soil-borne vascular pathogen, *Ralstonia solanacearum*, a rod-shaped gram-negative β-proteobacterium is the causal agent of bacterial wilt and is recognized as one of the most destructive plant bacterial pathogens worldwide (Genin 2010). It attacks more than 200 plant species, including many agriculturally important crops such as peanut, potato, tobacco, and banana (Hayward 1991), as well as the model plants, *Medicago truncatula* (Vailleau et al. 2007) and *Arabidopsis thaliana* (Deslandes et al. 1998). *R. solanacearum* GMI1000 has a large repertoire of 74 type III effectors; most of them remain functionally uncharacterized (Poueymiro and Genin 2009). Some of these proteins including GALA7, an effector containing an F-box and a Leu-rich repeat domain as well as AvrA, an HR (hypersensitive response) elicitor in tobacco, are required for host cell invasion (Turner et al. 2009).

R. solanacearum is also known to secrete several cell wall-degrading enzymes (CWDE) that are cellulolytic (Egl, CbhA, RSc0818, RSc1081) or pectinolytic (PglA/PehA, PehB, PehC, Pme) (Schell et al. 1988; Huang and Allen 1997; Tans-Kersten et al. 1998; Gonzalez and Allen 2003). In an elegant study based on combinatory mutations in the CWDE, 15 different strains were produced and their virulence in tomato plants was tested (Liu et al. 2005). Although the GMI-6 strain which was defective in all CWDE exhibited reduced virulence, cellulose rather than pectin degradation seemed to be more critical for *R. solanacearum* virulence in tomato (Liu et al. 2005). More recently, it has been demonstrated that *R. solanacearum* endo- and exo-PG are inhibited by a tomato polygalacturonase-inhibiting protein (PGIP) activity which may contribute to plant resistance to the pathogen (Schacht et al. 2011).

The infectious process of *R. solanacearum* has been described at the light microscopy level in tomato (Vasse et al. 1995, 2000; Wydra and Beri 2006, 2007), petunia (Zolobowska and Van Gijsegem 2006), and *Medicago truncatula* (Vailleau et al. 2007; Turner et al. 2009). In tomato and *M. truncatula*, bacteria penetrate the root at the apex with no preferential point of entry, as well as via sites of secondary root emergence (Vasse et al. 1995, 2000; Vailleau et al. 2007). In the case of in vitro-inoculated *M. truncatula* seedlings, the first symptoms were root growth arrest, root tip swelling, and epidermal cell death (Turner et al. 2009). Despite the fact that various aspects of the *R. solanacearum–A. thaliana* interaction have been well-characterized (Tasset et al. 2010), little is actually known about the mechanisms underlying *R. solanacearum* colonization in *A. thaliana* roots. During the compatible

interaction between the Col-0 ecotype and GMI1000 bacterial strain (plant–pathogen couple studied herein), it has been previously established that major changes in global gene expression associated with wilt disease development occur, at least in leaves (Hu et al. 2008).

Herein, we provide a detailed, cytological description of the *A. thaliana* Col-0 root system during a compatible interaction with *R. solanacearum* GMI1000. We describe how *R. solanacearum* enters the root apex, progresses through the intercellular spaces, and gains access to the vascular cylinder. In addition, double-labeling immunolocalization experiments using antibodies raised against different cell wall components in conjunction with Rsol-I, an antibody that recognizes *R. solanacearum* membrane lipopolysaccharides (LPS), allowed us to monitor *R. solanacearum*-induced, cell wall degradation dynamics leading to disease development.

Materials and methods

Plant material and growth conditions

Arabidopsis (*A. thaliana*) wild-type Col-0 (accession number N1093) used in this study is from NASC (Nottingham Arabidopsis Stock Centre). Seeds were germinated on Murashige and Skoog medium (Murashige and Skoog 1962) and placed in a growth chamber at 22/20 °C (day/night), with a 16-h light period and 40 % relative humidity. One week later, seedlings were transferred on Peters medium (Arancon et al. 2004) (2.5 g l^{-1}, supplemented with 10 g l^{-1} bacto agar) and Petri dishes were placed vertically in the same growth conditions.

Bacterial strain and pathogenicity assays

Ralstonia solanacearum strain GMI1000 was grown at 28 °C on BG medium (Plener et al. 2010). Inoculations with the bacterium were performed in vitro on 15-day-old seedlings by spotting 10 µl of bacterial suspension at an optical density at 600 nm of 0.01 (10^7 cfu/ml). Droplets were deposited 1 cm above the root apex.

Preparation of embedded sections for microscopy

Apical portions of roots were sampled from fresh, in vitro Arabidopsis seedlings and fixed overnight at 5 °C in 2.5 % (v/v) glutaraldehyde in 50 mM cacodylate buffer (pH 7.2). Fixed samples were rinsed three times in buffer and then dehydrated in a successive ethanol series (20, 40, 70, and 100 %) before impregnation in ethanol:LR White resin (Electron Microscopy Sciences), 33, 50, 66, and 100 % and embedding in gelatin capsules. The resin was polymerized overnight at 70 °C. Semi-thin sections of 1 µm (from ten different infected roots) were cut on an ultra-microtome (Ultracut E Reichtert) equipped with a diamond knife and mounted on multi-well slides for bright field observation or immunostaining. For transmission electron microscopy (TEM), ultra-thin sections (90 nm) from two selected infected roots were collected on gold grids.

Toluidine blue staining for light microscopy

Root sections were stained (1–2 min) with 0.05 % toluidine blue O (Sigma-Aldrich, St Louis, MO, USA) in 0.1 M $NaPO_4$ buffer (pH 7.0) at 70 °C on a hot plate, rinsed with deionized water, and air dried prior to observation with an inverted Leica microscope (Leitz DMIRBE). Images were recorded with a charge-coupled Device camera (Color Coolview, Photonic Science, UK).

Periodic acid-thiosemicarbazide-silver proteinate (PATAg) staining electron microscopy

Ultrathin cross sections were stained with PATAg test as described previously (Thiery 1967). Sections were incubated for 30 min in 1 % (w/v) periodic acid and rinsed twice in deionized water before 45 min of incubation in a 0.2 % (w/v) thiosemicarbazide solution in 20 % (v/v) acetic acid. After progressive rinsing in solutions with decreasing acetic acid concentration and then ultra pure water, grids were maintained 30 min in 1 % (w/v) silver proteinate in the dark, rinsed and then air-dried for observation with a JEOL JEM 1200 EX transmission electron microscope.

Immunocytochemistry

For confocal immunofluorescence studies, semi-thin sections were blocked in PBST–BSA (0.1 M phosphate-buffered saline, 2 % Tween, 1 % bovine serum albumin) for 2 h and labeled overnight (12 h) at 4 °C with primary antibody (PlantProbes, Leeds, UK) diluted as follows: LM6, and LM10 (1:10, v/v), and JIM7 (1:2, v/v). The *R. solanacearum*-specific primary antibody Rsol-I (Plant Research International, Wageningen, The Netherlands) was used at a dilution of 1:200 dilution (v/v). Sections were washed three times with PBST–BSA and incubated at room temperature for 2 h with a secondary antibody (goat anti-rat IgG for cell wall antibody detection, or goat-anti rabbit IgG for bacterial detection, coupled to the fluorescent dye Alexa Fluor 633 and 547, respectively (Molecular Probes) used at a 1:1000 (v/v) dilution in PBST–BSA. Samples were washed three times with PBST–BSA and then rinsed with ten drops of deionized water. Confocal microscopy images and fluorescent signal detection were acquired with

a Leica TCS SP2 AOBS confocal laser-scanning system equipped with an inverted microscope (Leica DM RXA2, Wetzlar, Germany) and a 63× oil immersion objective (numerical aperture 1.2). Autofluorescence was observed in the 590–650-nm spectral range. Samples were observed with the 488-nm line of an argon laser for excitation.

For TEM immunocytochemistry study, ultrathin sections were floated on PBST–BSA supplemented with 0.2 M glycine for 30 min to block non-specific binding. Sections were rinsed three times with PBST–BSA and three times with PBS before fixation in 0.5 % glutaraldehyde. After washing three times with PBS and three times with ultra pure water, grids were air dried before observation with a JEOL JEM 1200 EX transmission electron microscope.

Bioinformatic search for pathogens cell wall-degrading enzymatic enzymes

A keyword-based search for cell wall polysaccharide-modifying and degrading enzymes was performed on the MaGe database (Magnifying Genomes; http://www.genoscope.cns.fr/agc/mage) which contains gene annotations for many bacterial genomes (Vallenet et al. 2006) and a database specifically dedicated to genomic sequences of *R. solanacearum* strains (http://iant.toulouse.inra.fr/bacteria/annotation/cgi/ralso.cgi). Based on gene annotations, protein sequences for cell wall-modifying and degrading enzymes from another bacterial vascular pathogen, *Xanthomonas campestris* pv. *Campestris*, were retrieved (da Silva 2002) and used in blast analyses of *R. solanacearum* strain genomes.

Results

Ralstonia solanacearum colonizes the roots of in vitro-grown Arabidopsis seedlings

Arabidopsis Columbia (Col-0) plants were used to study the compatible interaction that occurs when infected with the *R. solanacearum* GMI1000 strain. In vitro-grown, 15-day-old seedlings were inoculated by depositing a drop of bacterial suspension on the primary root close to the apex (Fig. 1). Whereas primary and lateral roots developed in mock-inoculated (water) seedlings (Fig. 1a), *R. solanacearum*-inoculated roots were characterized by growth arrest of the primary root and an absence of lateral root formation (Fig. 1b). Within 18 days post-inoculation (dpi), the infected plants wilted, became chlorotic, and died (Fig. 1b).

R. solanacearum provokes plasmolysis of epidermal and cortical root cells and moves directly to the vascular cylinder via intercellular spaces

Transverse sections of roots prior to and during infection were observed at the light microscopy level (Fig. 2). The architecture (organization and cell number) of the Arabidopsis root is highly invariable which allows for the unambiguous identification and characterization of the different cell types during infection (Fig. 2a). Compared with non-inoculated seedlings (Fig. 2a), infected roots at 2 dpi exhibited a generalized plasmolysis of epidermal, cortical, and endodermal cells (Fig. 2b; Supplemental Fig S1). Within 6 dpi, the epidermal cells appeared collapsed and a "bacterial pocket" was observed in the endodermal/pericycle junction in alignment with one of the xylem pole axes (Fig. 2c). At a late stage of disease development (15 dpi), bacteria were abundant in the vascular cylinder to the point where several of the xylem vessels were completely filled with bacteria (Fig. 2d). Based on these results, we focused our attention on 6 dpi roots for further characterization of the compatible *R. solanacearum–A. thaliana* interaction.

To further characterize the presence of bacteria throughout the root during infection, immunolocalisation experiments using Rsol-I, an antibody that specifically labels membrane lipopolysaccharides (LPS) of *R. solanacearum*, were performed (Fig. 3). At 6 dpi, bacteria tended to have a highly restricted localization with bacteria present in a few epidermal cells infected (in this case only one), with a slightly broader colonization in cortical and endodermal cells (3–4 cells) (Fig. 3a, b). In these cells, bacteria were localized in the periplasm (between the cell wall and the plasmolyzed plasma membrane) and never observed in the protoplasm (Fig. 3c). Interestingly, compared with the generalized plasmolysis observed throughout the root at this stage of infection, relatively few cells actually appeared to be in direct contact with the bacteria. These findings suggest that *R. solanacearum* joins the xylem pole as directly as possible, rather than massively colonizing all the different cell types along its path.

In tomato and *M. truncatula* roots, *R. solanacearum* moves towards the vascular cylinder via intercellular spaces (Vasse et al. 1995; Vailleau et al. 2007). To determine if this is the case in Arabidopsis, TEM was used to examine the progression of *R. solanacearum* near the root apex (Fig. 4). In Fig. 4a, one bacterial cell was visible in the intercellular space between two epidermal cells and another between two cortical cells and an endodermal cell. A close-up of the latter zone indicated locally digested cell walls of the adjacent cortical and endodermal cells (Fig. 4b). Cell wall degradation was minimal, presumably because bacteria do not appear to readily multiply in these

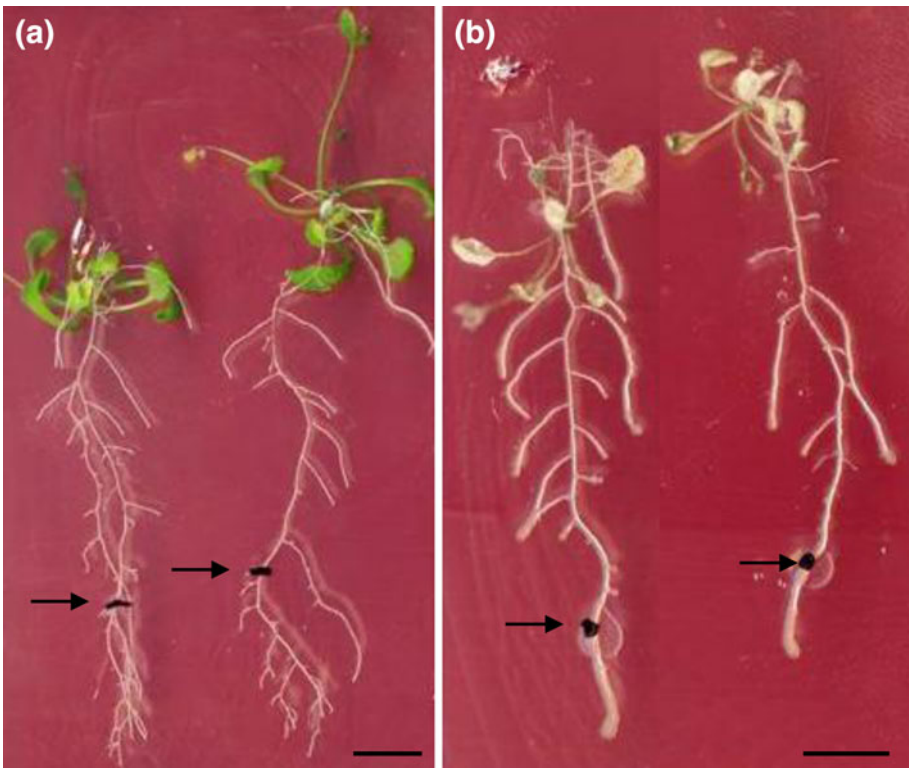

Fig. 1 The compatible *Ralstonia solanacearum* GMI1000/*Arabidopsis thaliana* Col-0 interaction in an in vitro pathosystem. Arabidopsis Col-0 seedlings were grown for 15 days in vitro and then mock-inoculated with water (**a**) or inoculated with *Ralstonia solanacearum* GMI1000 (**b**). *Black arrows* indicate primary root tips where water (mock) or bacteria droplets were deposited. Photographs were taken 18 days post inoculation (dpi). Note root growth arrest in the presence of the bacterium (**b**). Magnification *bar* 1 cm

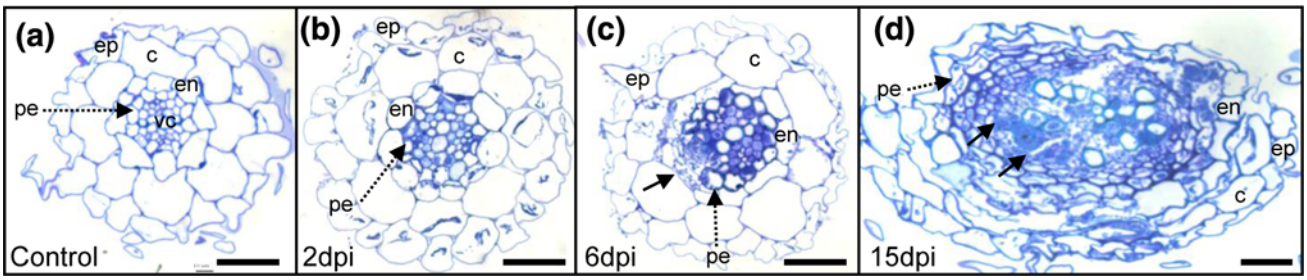

Fig. 2 Overview of *Ralstonia solanacearum* colonization of the *Arabidopsis* root. Transverse root sections were stained with toluidine blue. **a** Roots prior to inoculation. Inoculated roots at 2 dpi (**b**), 6 dpi (**c**), and 15 dpi (**d**). *Arrows* indicate the bacterial pocket and xylem vessels filled with bacteria (**c** and **d**, respectively). *ep* epidermis, *c* cortical cell, *vc* vascular cylinder, *en* endoderm, *pe* pericycle. Magnification *bar* 50 µm

intercellular spaces. Further inward, TEM observations revealed the occurrence of numerous bacteria in the intercellular space between the endodermis and the pericycle (Fig. 4c). These results suggest that the intercellular spaces in close proximity to the vascular cylinder constitute a particularly favorable environment for *R. solanacearum*.

R. solanacearum enters the vascular cylinder between two pericycle cells located at the xylem pole and multiplies profusely in xylem vessels

A critical step in vascular pathogen invasion is the entry into the xylem vessels. In Arabidopsis roots, protoxylem vessels are localized immediately inward of two xylem pole pericycle cells, which are, in turn, directly inward of one endodermal cell (Dolan et al. 1993). Using TEM, we focused our attention on this zone which corresponds to the "bacterial pocket" observed in bright field microscopy (Fig. 2c). *R. solanacearum* provoked the enlargement of the endodermal cell to the point of cell wall rupture which in turn resulted in an increased area between the endodermal and pericycle cells for bacterial multiplication (Fig. 5a, b). As for the pericycle cells, the only ones affected by the bacteria were those located at the xylem pole and in direct contact with the bacterial pocket (Fig. 5a). These pericycle cells appeared shrunken and collapsed (Fig. 5c). The adjacent pericycle cells (Fig. 5a) or those at the opposite xylem pole axis (Fig. 5d) remained intact. The lack of generalized plasmolysis throughout the pericycle (and the majority of the cells within the vascular

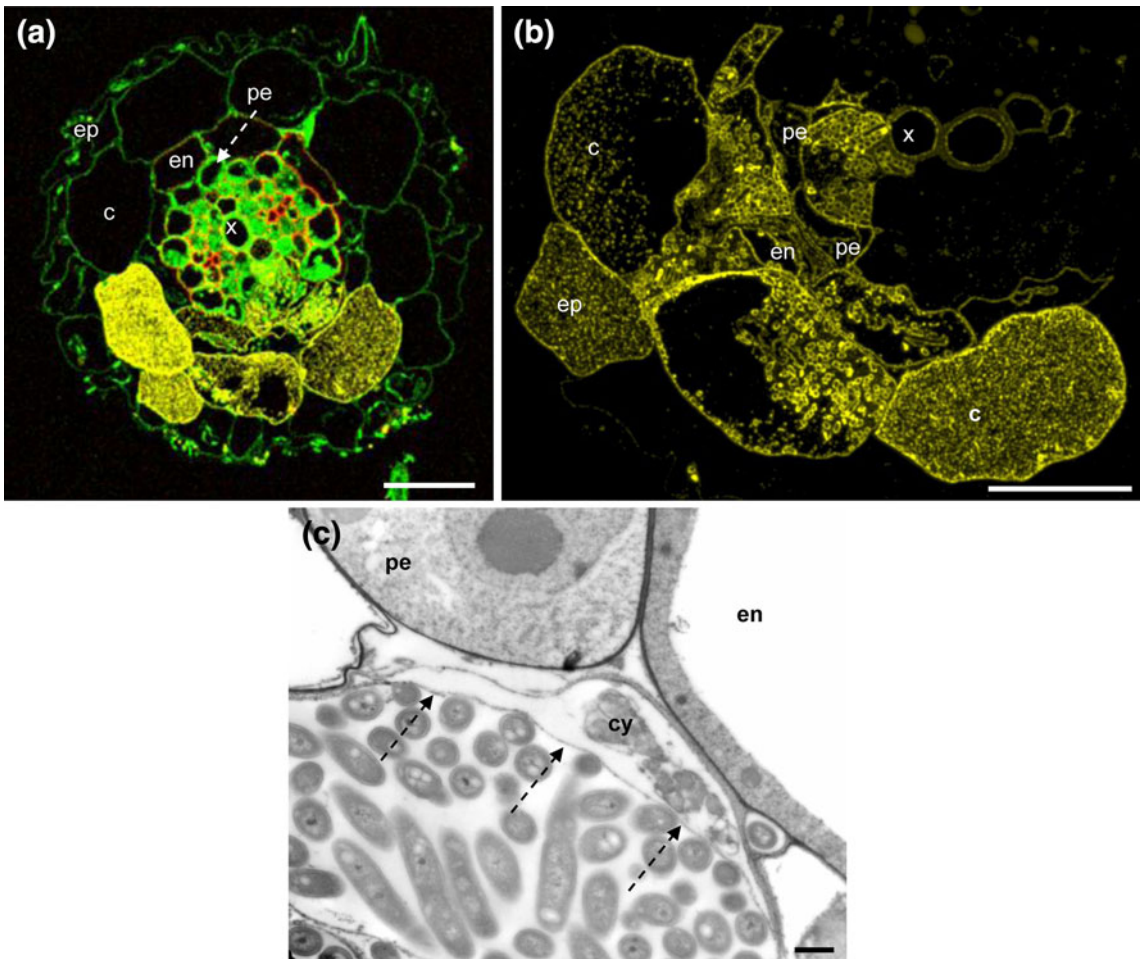

Fig. 3 Localisation of *Ralstonia solanacearum* GMI1000 in 6 dpi roots. **a** Confocal image of transverse root section. Bacteria are immunolabeled with Rsol-I antibody in *yellow*. Plant cell wall autofluorescence is visualized in *green*. **b** Serial section and higher magnification of the infected zone of the root section in **a**. **c** Distribution of *R. solanacearum* inside an infected endodermal cell. As determined by TEM, bacteria are localized the periplasm, but not inside the protoplasm. *Dashed arrows* plasma membrane. *ep* epidermis, *c* cortical cell, *cy* condensed cytoplasm, *en* endodermis, *pe* pericycle, *x* xylem vessel. Magnification *bars*: 25 μm (**a**, **b**), 0.5 μm (**c**)

cylinder) (Fig. 5a) suggests different cellular responses to *R. solanacearum* on either side of the pericycle.

Once inside the protoxylem vessels, *R. solanacearum* readily multiplied (Fig. 5e). Since the rod-shaped bacteria appeared transversally sectioned in root cross sections, this implies that they were mainly oriented in parallel to the flow of the xylem sap. In serial root sections taken above the entry point of *R. solanacearum* into the vascular cylinder, bacteria were confined to the xylem vessels and provoked little to no deleterious effects to the surrounding cells (Fig. 5f). This observation suggests that once the bacteria colonize the vascular cylinder, they are contained there with little subsequent lateral movement back outward. At 6 dpi, bacteria were not detected in the phloem (Fig. 5g).

At a later stage of infection (15 dpi), bacteria extensively invaded xylem vessels and proliferated from vessel to vessel after digestion of the pit membrane (Fig. 6). Bacteria also multiplied in zones corresponding to xylem parenchyma corpses, resulting in enlarged intercellular spaces between necrotic cells. At this stage, the phloem remained free of bacterial invasion.

R. solanacearum differentially degrades plant cell wall components in a tissue-specific manner

The description of pathogen ingress in *Arabidopsis* was completed by monitoring *R. solanacearum*-induced cell wall changes in the root during infection. Immunolocalization experiments were performed using monoclonal antibodies that specifically recognize different carbohydrate epitopes of plant cell walls (Fig. 7). We first examined the distribution of methyl-esterified pectic homogalacturonan (HG) with JIM7 antibodies in uninfected roots (Fig. 7a) and

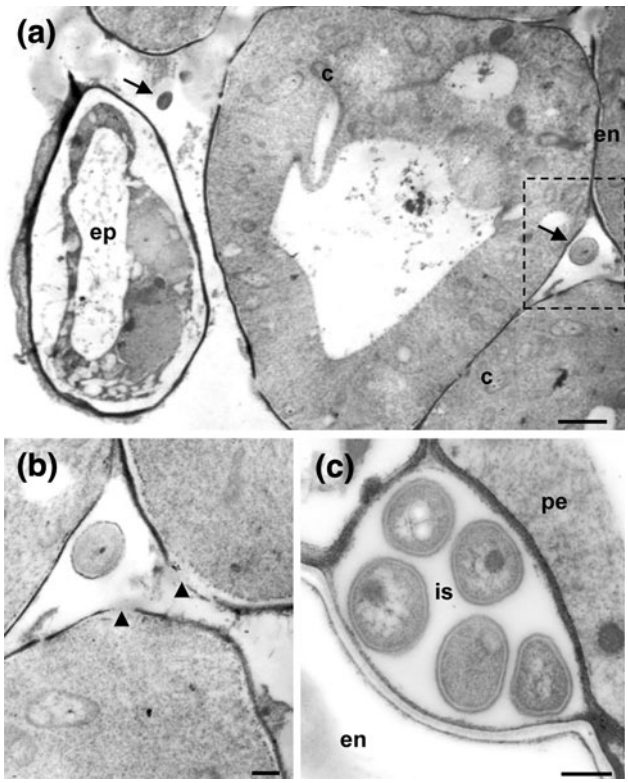

Fig. 4 *Ralstonia solanacearum* in intercellular spaces throughout the cortex. TEM observations of transverse sections of *Arabidopsis* roots at 6 dpi. **a** *R. solanacearum* are present in intercellular spaces between epidermal and cortical cells, and cortical and endodermal cells (*arrows*). **b** Close-up of the *boxed area* in **a**. Localized cell wall degradation (*arrowheads*) of cortical and endodermal cells adjacent to the intercellular space is observed. **c** Bacterial proliferation in an intercellular space between an endodermal and pericycle cell. *c* cortical cell, *en* endodermal cell, *ep* epidermal cell, *pe* pericycle, *is* intercellular space. Magnification *bars*: 1 μm (**a**), 500 nm (**b**, **c**)

roots at 6 dpi (Fig. 7b). In the absence of pathogen, cell walls were uniformly labeled with JIM7 throughout the root (Fig. 7a). At 6 dpi, all cortical cells, either directly in contact with *R. solanacearum* or not, were no longer labeled with JIM7, suggesting a global de-methylesterification of cell wall pectins throughout the cortex (Fig. 7b). Similar results were observed with JIM5 antibodies which recognize unmethylesterified and weakly methyl-esterified HG (data not shown), thereby suggesting an overall degradation, and not just a de-methylesterification of pectic HG in the cortex.

In uninfected roots, anti-arabinan LM6 epitopes were mainly localized in cells within the vascular cylinder (Fig. 7c). The presence of *R. solanacearum* did not significantly alter the LM6 labeling at 6 dpi (Fig. 7d) or 15 dpi (data not shown). Higher magnification, serial sections of the vascular cylinder labeled with either JIM7 (Fig. 7e, g) or LM6 (Fig. 7f) were then observed. HG pectin was efficiently degraded in all cell walls in direct contact with the bacteria as illustrated by double immunolabeling with JIM7 and Rsol-I antibodies (Fig. 7g). On the contrary, several cell walls in direct contact with *R. solanacearum* retained LM6 label, suggesting less efficient bacterial arabinan degradation as compared with HG pectin (Fig. 7f).

Finally, since xylem vessels have secondary walls, we also determined the effect of *R. solanacearum* on xylan, a major component of secondary walls, using an LM10 anti-xylan antibody (Fig. 7h–j). In uninoculated roots, LM10 label was exclusively localized in the secondary cell walls of xylem vessels (Fig. 7h). At 15 dpi, despite the fact that xylem vessels were filled with bacteria, LM10 labeling was still intense in xylem vessels (Fig. 7j). These results suggest that although there is direct contact between xylan and bacteria, *R. solanacearum* does not appear to be able to efficiently degrade xylan and that xylan degradation is not essential for vessel colonization.

The enzymatic arsenal of *R. solanacearum* may govern the selective degradation of plant cell wall components

Based on immunolocalization data, the progression of *R. solanacearum* within the Arabidopsis root does not require complete degradation of plant cell walls and there is a certain degree of specificity in terms of the different wall components the bacteria can efficiently degrade. We sought to determine if there was correlation between the theoretical ability of the pathogen to degrade the plant wall and these microscopy observations. Towards this end, we searched the MaGe database (Magnifying Genomes; http://www.genoscope.cns.fr/agc/mage) which contains gene annotations for many bacterial genomes (Vallenet et al. 2006) and a database specifically dedicated to genomic sequences of *R. solanacearum* strains (http://iant.toulouse.inra.fr/bacteria/annotation/cgi/ralso.cgi). A cell wall-related, keyword-based search was first performed on the GM1000 genome. Eight wall-degrading enzymes in *R. solanacearum* have been previously described: three glucanases, a glucosidase, a pectinmethylesterase, and three polygalacturonases (Schell et al. 1988; Huang and Allen 1997; Tans-Kersten et al. 1998; Gonzalez and Allen 2003), and only these sequences of pectinolytic and cellulolytic function could be retrieved in this manner (Supplemental Table S1). In keeping with microscopy data, no hits were identified when using xylanase, xylosidase, arabinofuranosidase, or arabinanase as keywords. Searching the five other *R. solanacearum* strain genomes did not allow us to identify any additional putative cell wall genes in this manner. Since this approach is based on reliable annotations, a complementary approach was employed.

Xanthomonas campestris pv. *campestris* (*Xcc*), another bacterial vascular pathogen, has at least 40 putative

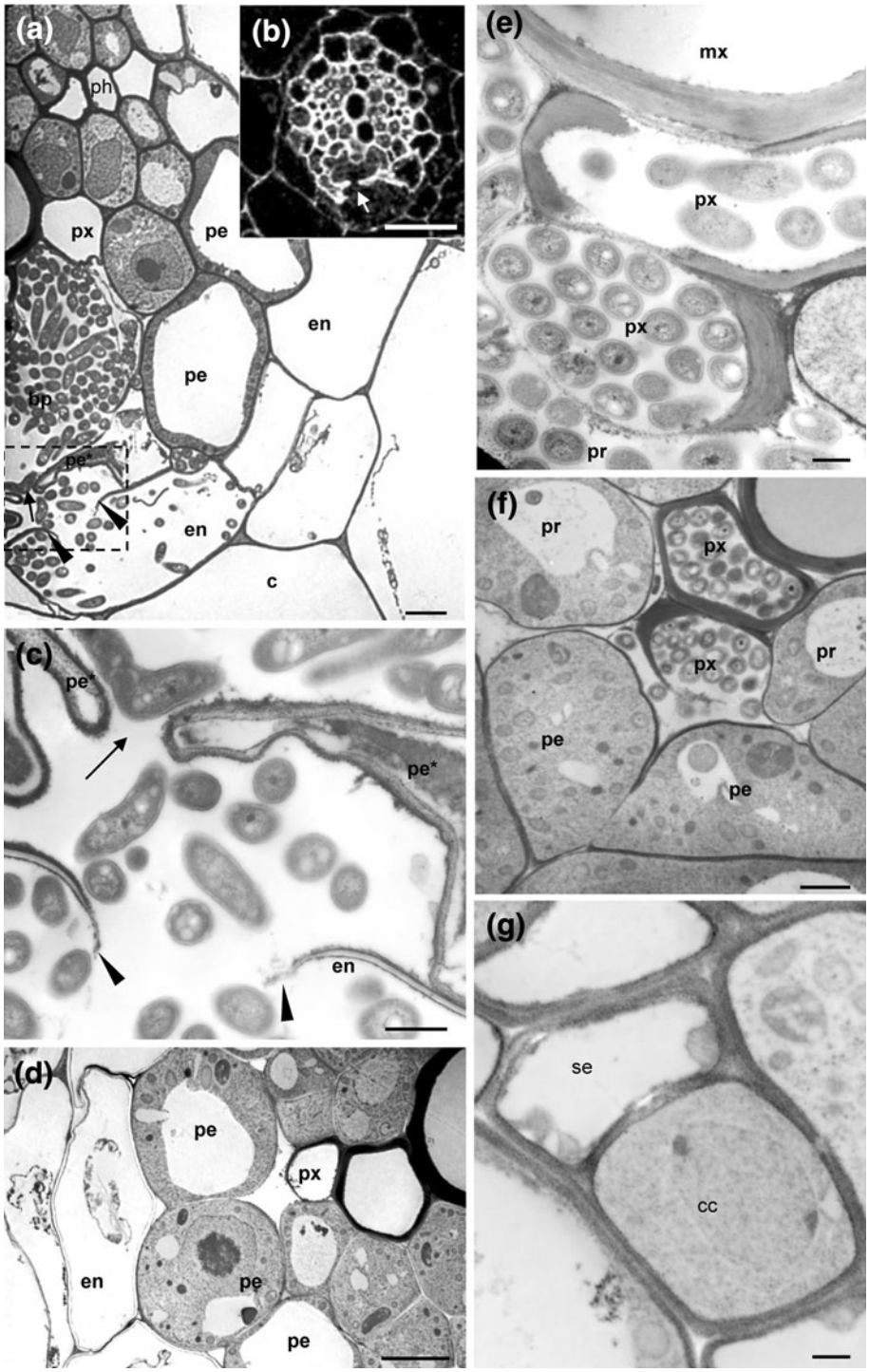

wall-degrading enzymes in its genome (da Silva 2002). These sequences were retrieved and used to perform blast searches on the *R. solanacearum* genome. Beyond the previously identified eight cell wall genes, none of the other *Xcc* gene sequences exhibited significant sequence homology with *R. solanacearum* sequences (data not shown). These data suggest that the apparent specificity of cell wall degradation patterns observed in Arabidopsis roots may be governed by the arsenal of enzymes that *R. solanacearum* possesses in its genome.

◀ **Fig. 5** *R. solanacearum* enters the vascular cylinder between two pericycle cells located at the xylem pole. **a**, **c**–**g** TEM observations of transverse sections of 6 dpi *Arabidopsis* roots. **a** Focus on the bacterial pocket. The bacterial pocket is formed by the fusion of degenerated procambial cells. Except for the pericycle cells at the xylem pole (pe*), all other pericycle cells show no show signs of plasmolysis. The endodermal cell wall is ruptured (*arrowheads*). **b** Overview of 6 dpi root. Bacteria entry into the vascular cylinder as a result of xylem pole pericycle cell collapse is indicated (*arrow*). **c** Close up of boxed-in area in **a**. Note cell wall rupture of the infected endodermal cell (*arrow*) and bacteria invasion of the intercellular space between the endodermis and the two collapsed xylem pole pericycle cells (pe*). *Arrows* in **a**, **b**, and **c** indicate the entry point of bacteria into the vascular cylinder. **d** General view of the same infected root at the xylem pole opposite from the bacterial pocket. Note the absence of bacteria. Endodermal and cortical cell plasmolysis is observed, but pericycle cells appear viable. **e** Protoxylem vessels filled with bacteria. **f** Serial section taken above the bacterial entry point. Note that bacteria are restricted to xylem vessels and that pericycle and procambial cells do not appear to be affected by the presence of *R. solanacearum*. **g** The phloem remains free from bacterial infection. *c* cortical cell, *en* endodermis, *pe* pericycle, *px* protoxylem vessel, *mx* metaxylem vessel, *bp* bacterial pocket, *pr* procambial cell, *ph* phloem, *se* sieve element, *cc* companion cell. Magnification *bars*: 10 μm (**a**, **d**); 50 μm (**b**); 1 μm (**c**, **e**); 2 μm (**f**, **g**)

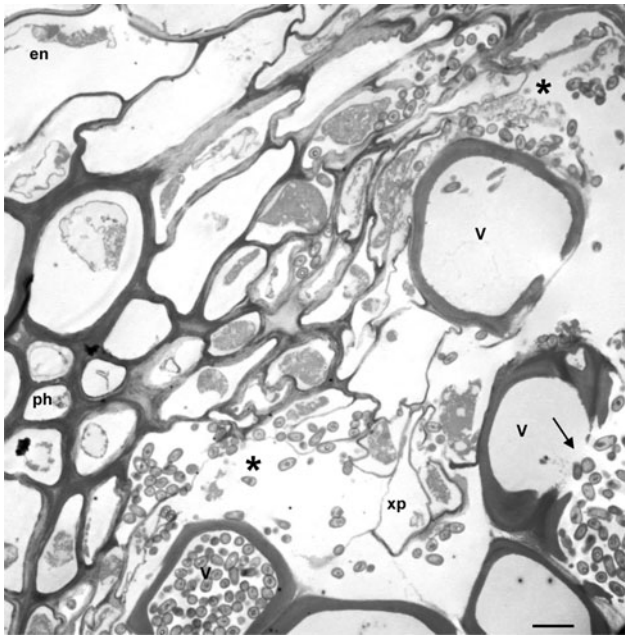

Fig. 6 *R. solanacearum* thrives in the xylem. TEM of transverse sections of 15 dpi *Arabidopsis* roots. Note bacterial multiplication in vessels and digestion of the pit membrane between vessels (*arrow*). Bacteria proliferate in necrotic cells and in enlarged spaces between collapsed cells (*asterisks*). At this late stage during disease development, phloem cells are not infected. *en* endodermis, *ph* phloem, *v* vessel, *xp* xylem parenchyma. Magnification *bar* 10 μm

Discussion

Specificities of *R. solanacearum* ingress into the Arabidopsis root

Optical and electron microscopy has been previously employed to describe the anatomy of the primary root in *Arabidopsis* and it is characterized by its simplicity and quasi-invariance in cell patterning and number (Dolan et al. 1993). These characteristics were conserved in in vitro-grown *Arabidopsis* seedlings, thereby facilitating the interpretation of the cellular events occurring during the *R. solanacearum*–Arabidopsis compatible interaction. Based on the data compiled in this study, a model indicating the most probable route of *R. solanacearum* colonization of a Col-0 *Arabidopsis* root is proposed (Fig. 8).

Upon infection, bacteria must penetrate the root surface. In tomato seedlings, *R. solanacearum* requires wound sites or natural openings at the point of secondary root emergence or partially exfoliated cells of the outer parenchyma (Saile et al. 1997). Our observations suggest that infection of in vitro-grown, seedlings did not require root lesion for entry. We demonstrated that bacteria can penetrate into the root between epidermal cells at the root apex. The infectious process requires the centripetal movement of the bacteria through intercellular spaces to reach their final destination where bacteria multiply: the xylem vessels (Fig. 8). Root pathogens often take advantage of intercellular spaces to multiply. In tomato and *M. truncatula* roots, *R. solanacearum* readily multiplies in the intercellular spaces of the cortex (Vasse et al. 1995; Vailleau et al. 2007). In our study, we show that although *R. solanacearum* does move through cortical intercellular spaces, it does not particularly thrive there. Bacteria in the periplasm of plasmolyzed epidermal and cortical cells were also occasionally observed. In tomato, some epidermal cells were also filled with bacteria (Vasse et al. 1995).

R. solanacearum induces plasmolysis and pectin degradation throughout the Arabidopsis root cortex

Despite the fact that relatively few cortical cells were in contact with the bacteria as indicated by Rsol-I immunolabeling experiments, plasmolysis throughout the cortex was observed. Extensive plasmolysis of the root cortex has also been reported in *R. solanacearum*-infected tomato roots (Vasse et al. 2000). The induction of plasmolysis away from the infected zone may be dependent on intercellular signaling mechanisms. Upon infection, pectin degradation was also apparent throughout the root cortex, even in those cells that were not directly exposed to the bacteria. Similar observations have been reported in the cocoyam–*Pythium myriotylum* host–pathogen interaction (Boudjeko et al. 2006). Using the JIM7 antibody, the

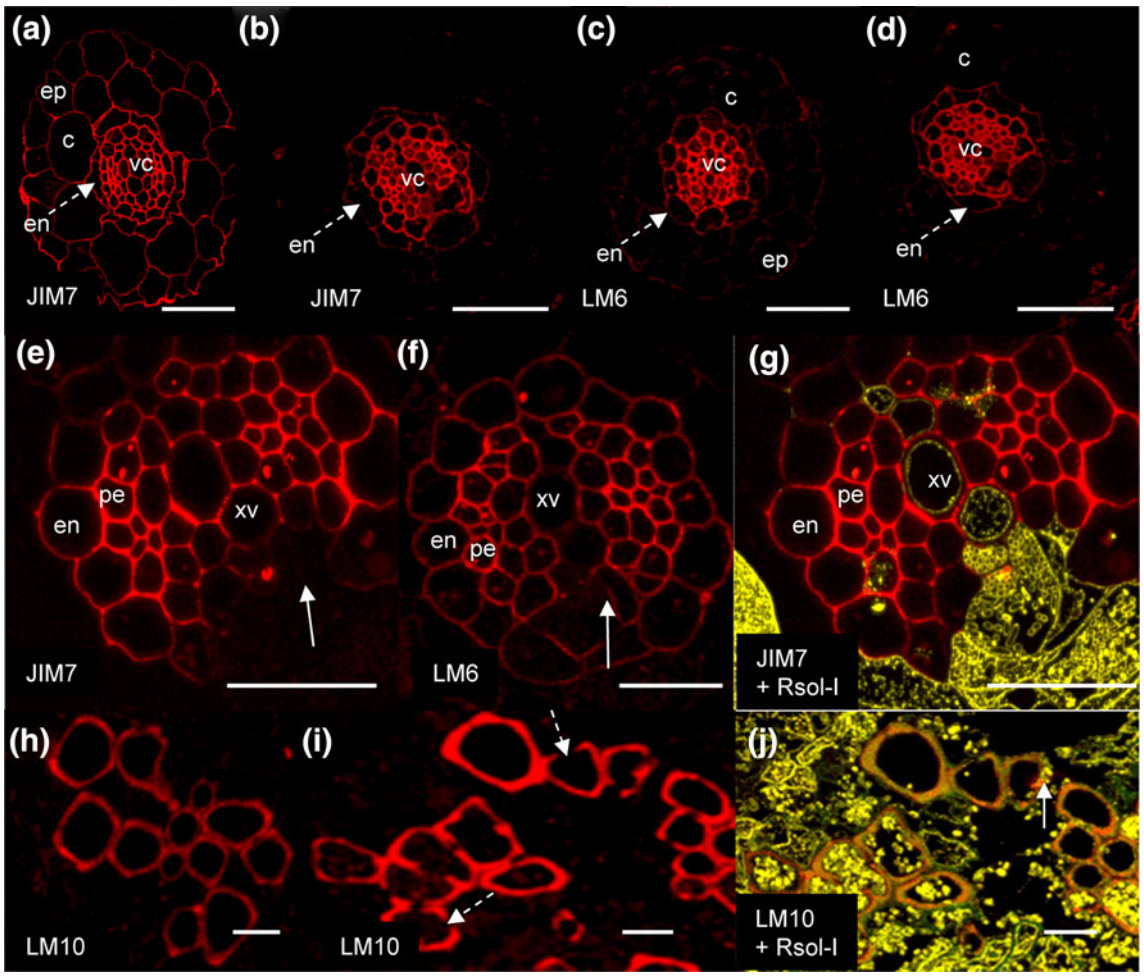

Fig. 7 *R. solanacearum* differentially degrades plant cell wall components in a tissue-specific manner. **a** HG (homogalacturonan) epitopes (JIM7 antibodies) are localized in all cell walls of non-inoculated roots. **b** At 6 dpi, HG (JIM7) labeling is exclusively in the vascular cylinder. Arabinan (LM6) labeling of non-infected root (**c**) and infected (**d**) at 6 dpi. Serial sections stained with JIM7 (**e**), LM6 (**f**), or double-labeled with JIM7 (*red*) and Rsol-I (*yellow*) (**g**). Note cell walls (see *arrows*) labeled with LM6 (**f**), but not with JIM7 (**e**). Xylan (LM10) labeling in secondary walls of xylem vessels in non-inoculated (**h**), 15 dpi (**i**), or double-labeled (**j**) with LM10 (*red*) and Rsol-I (*yellow*). Note the pits (*dashed arrows*) in **i**. *c* cortical cell, *en* endodermal cell, *ep* epidermal cell, *pe* pericycle, *vc* vascular cylinder, *xv* xylem vessel. Magnification *bars*: 50 μm (**a**–**d**); 25 μm (**e**–**g**); 10 μm (**k**–**j**)

authors showed that as soon as the fungus came in contact with the epidermal cells of the root apex, it caused a significant loss of pectin in cortical cells far from the contact zone with the pathogen (Boudjeko et al. 2006). Similarly, *Pythium ultimum* provoked pectin degradation in carrot roots, even at a relatively long distance from the fungal hyphae (Campion et al. 1998).

During plant–pathogen interactions, pectin degradation products such as (1–4)-α-linked oligogalacturonides (OG) have been shown to elicit various plant defense responses (Aziz et al. 2004, 2007), with highly methylesterified pectins as the source of the most active host elicitors (Osorio et al. 2008; Curvers et al. 2010). For example, genotypes of tomato that were resistant to *R. solanacearum* were characterized by pectins with a high degree of methyl-esterification (Wydra and Beri 2006, 2007). *R. solanacearum* secretes several extracellular plant cell wall-degrading enzymes (CWDE) via the type II secretion system (Poueymiro and Genin 2009). It possesses several pectin-degrading enzymes including a pectin methylesterase (PME) which cleaves methoxyl groups from methylated pectin, thereby making them susceptible to the three polygalacturonases: PehA/PglA, PehB, and PehC (Tans-Kersten et al. 1998). Besides this suite of enzymes, bioinformatic searches indicated that *R. solanacearum* is not particularly rich in wall-degrading enzymes compared with other phytopathogenic bacteria (da Silva 2002). It is possible that cell wall-derived pectic fragments of root cortical cells may induce programmed cell death in the entire cortex, even at a distance from bacterial exposure.

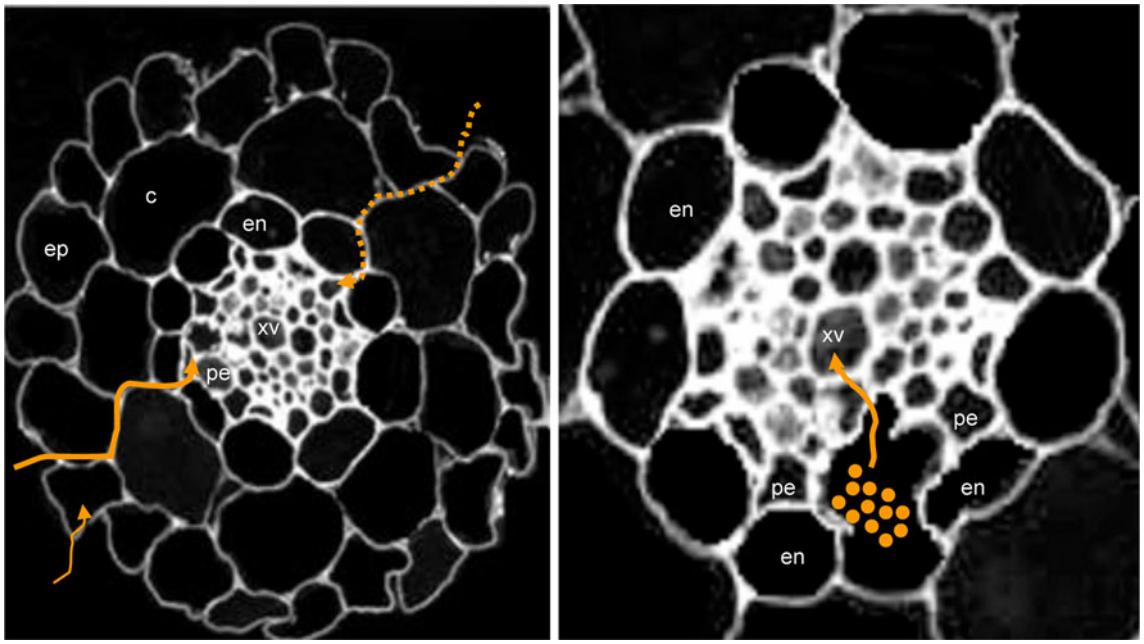

Fig. 8 Schema of *R. solanacearum* colonization of the Arabidopsis root during a compatible interaction. *R. solanacearum* exhibits two phases of infection in the root: a propagation phase (*left panel*) and a proliferation phase (*right panel*). The propagation phase occurs within the cortex (*thick solid arrow*) with bacteria principally observed in the intercellular spaces. Bacteria are also observed, albeit in a highly restricted manner, in plasmolysed epidermal cells (*thin solid arrow*). Another potential propagation route is also indicated (*dashed arrow*). In a second phase (*right panel*), when the bacteria reach the endodermal/pericycle cell junction facing the xylem pole, bacterial proliferation begins and massive invasion is observed in the xylem vessels. *ep* epidermal cell, *c* cortical cell, *en* endodermis, *pe* pericycle, *xv* xylem vessel

This implies that *R. solanacearum*-mediated, pectin hydrolysis would result in the activation of defense in non-infected cells. In contrast, in the vascular cylinder, pectins were only degraded in infected cells by *R. solanacearum*. In tomato stem extracts, PGIP activity against *R. solanacearum* PGs has been reported (Schacht et al. 2011). It is conceivable that Arabidopsis produces an equivalent PGIP in the vascular cylinder, provoking the depolymerisation of elicitor-active oligogalacturonides to inactive molecules.

The pericycle cells at the xylem poles play a key role in *R. solanacearum* invasion

In contrast to the generalized response to the bacteria in epidermal and cortical cells, only the pericycle cells located at the xylem poles undergo cell collapse whereas the other pericycle cells remain viable. To circumvent basal defenses and successfully colonize its host, *R. solanacearum* encodes type III effectors (T3E) which are injected into the plant cell through a syringe-like apparatus called the type three secretion system and contribute to pathogen multiplication and pathogenicity (Alfano and Collmer 2004; Angot et al. 2006). *R. solanacearum* T3E subverts host cellular pathways, either by mimicking the action of key host proteins or by inducing their subcellular relocalization (Poueymiro and Genin 2009). The HR-like response observed may be caused by some bacterial effectors that possess necrotic activities and may trigger cell death in the pericycle cells at the xylem pole to facilitate its entry into the vascular cylinder. Indeed, some extracellular bacterial proteins, such by PopA1 and its derivative PopA3, can act as hypersensitive-like response elicitors both in tobacco and petunia although their cell-type specificity has not been yet addressed (Arlat et al. 1994). Furthermore, the intercellular space between the endodermal and xylem pole pericycle cells contains numerous bacteria that may potentially deliver effectors into these pericycle cells. Interestingly, it has been previously reported that xylem pole pericycle cells have several features that distinguish them from the other pericycle cells: they are shorter and differ in cytological content, display meristematic features, and are competent to initiate lateral root development (De Smet et al. 2006; Dubrovsky et al. 2008; Parizot et al. 2008). Future studies should be carried out to decipher the mechanisms underlying xylem pole pericycle cell death and the highly directional movement of the bacteria towards these cells from the root surface.

Finally, once *R. solanacearum* succeeds in entering the vascular cylinder, basal plant defense in the Arabidopsis root is much less efficient (or inexistent) in inhibiting

extensive bacterial multiplication. In the Arabidopsis–*R. solanacearum* compatible interaction reported herein, the bacteria readily multiplied in xylem vessels and moved from vessel to vessel via degenerated pit membranes. Similarly, in stems of tomato cultivars that were susceptible to *R. solanacearum*, bacterial readily spread from vessel to vessel through degenerated pit membranes (Nakaho et al. 2000). However, in resistant tomato cultivars, pit membranes were thicker, electron-dense, resulting in limited bacterial movement (Nakaho et al. 2000). These results indicate that xylem vessel structure can also participate in dictating plant response to vascular pathogens.

In conclusion, our study provides the first cellular description of the compatible interaction between the model plant Arabidopsis Col-0 and the phytopathogenic bacterium, *R. solanacearum* GMI1000. This is surprising in light of the fact that this pathosystem was developed nearly 15 years ago (Deslandes et al. 1998). Beyond documenting the progression of the bacteria in the root, we focused on the cell-type specific, plant cell wall modifications occurring during disease development. Our work opens new avenues in the understanding of plant–vascular pathogen interactions and revealed a key role for the cortical and pericycle cells in determining the outcome the Arabidopsis–*R. solanacearum* interaction and may help to define other root vascular pathogen invasion strategies.

Acknowledgments The authors would like to thank Stéphane Genin and Alice Guidot (LIPM, Toulouse, France) for helpful discussions, and Françoise Poliakoff, Corrine Audusseau and Carène Rivoal (ANSES-Laboratoire de la Santé des Végétaux, Angers, France) for the generous gift of Rsol-I antibody. This work was funded by the French National Agency for Research (WALLTALK: ANR-07-GPLA-014).

References

Alfano JR, Collmer A (2004) Type III secretion system effector proteins: double agents in bacterial disease and plant defense. Annu Rev Phytopathol 42:385–414

Angot A, Peeters N, Lechner E, Vailleau F, Baud C, Gentzbittel L, Sartorel E, Genschik P, Boucher C, Genin S (2006) *Ralstonia solanacearum* requires F-box-like domain-containing type III effectors to promote disease on several host plants. Proc Natl Acad Sci USA 103:14620–14625

Arancon NQ, Edwards CA, Atiyeh R, Metzger JD (2004) Effects of vermicomposts produced from food waste on the growth and yields of greenhouse peppers. Bioresour Technol 93:139–144

Arlat M, Van Gijsegem F, Huet JC, Pernollet JC, Boucher CA (1994) PopA1, a protein which induces a hypersensitivity-like response on specific *Petunia* genotypes, is secreted via the Hrp pathway of *Pseudomonas solanacearum*. EMBO J 13:543–553

Aziz A, Heyraud A, Lambert B (2004) Oligogalacturonide signal transduction, induction of defense-related responses and protection of grapevine against *Botrytis cinerea*. Planta 218: 767–774

Aziz A, Gauthier A, Bezier A, Poinssot B, Joubert JM, Pugin A, Heyraud A, Baillieul F (2007) Elicitor and resistance-inducing activities of beta-1,4 cellodextrins in grapevine, comparison with beta-1,3 glucans and alpha-1,4 oligogalacturonides. J Exp Bot 58:1463–1472

Blanvillain S, Meyer D, Boulanger A, Lautier M, Guynet C, Denancé N, Vasse J, Lauber E, Arlat M (2007) Plant carbohydrate scavenging through Tonb-dependent receptors: A feature shared by phytopathogenic and aquatic bacteria. PLoS One 2:e224

Boudjeko T, Andème-Onzighi C, Vicré M, Balangé A-P, Ndoumou DO, Driouich A (2006) Loss of pectin is an early event during infection of cocoyam roots by *Pythium myriotylum*. Planta 223:271–282

Burton RA, Gidley MJ, Fincher GB (2010) Heterogeneity in the chemistry, structure and function of plant cell walls. Nat Chem Biol 6:724–732

Campion C, Vian B, Nicole M, Rouxel F (1998) A comparative study of carrot root tissue colonization and cell wall degradation by *Pythium violae* and *Pythium ultimum*, two pathogens responsible for cavity spot. Can J Microbiol 44:221–230

Carpita NC (2011) Update on mechanisms of plant cell wall biosynthesis: how plants make cellulose and other (1 → 4)-{beta}-D-glycans. Plant Physiol 155:171–184

Cosgrove DJ (2005) Growth of the plant cell wall. Nat Rev Mol Cell Biol 6:850–861

Curvers K, Seifi H, Mouille G, de Rycke R, Asselbergh B, Van Hecke A, Vanderschaeghe D, Hofte H, Callewaert N, Van Breusegem F, Hofte M (2010) Abscisic acid deficiency causes changes in cuticle permeability and pectin composition that influence tomato resistance to *Botrytis cinerea*. Plant Physiol 154:847–860

da Silva AC (2002) Comparison of the genomes of two *Xanthomonas* pathogens with differing host specificities. Nature 417:459–463

De Smet I, Vanneste S, Inze D, Beeckman T (2006) Lateral root initiation or the birth of a new meristem. Plant Mol Biol 60: 871–887

Deslandes L, Pileur F, Liaubet L, Camut S, Can C, Williams K, Holub E, Beynon J, Arlat M, Marco Y (1998) Genetic characterization of *RRS1*, a recessive locus in *Arabidopsis thaliana* that confers resistance to the bacterial soilborne pathogen *Ralstonia solanacearum*. Mol Plant Microbe Interact 11:659–667

Dolan L, Janmaat K, Willemsen V, Linstead P, Poethig S, Roberts K, Scheres B (1993) Cellular organisation of the *Arabidopsis thaliana* root. Development 119:71–84

Dubrovsky JG, Sauer M, Napsucialy-Mendivil S, Ivanchenko MG, Friml J, Shishkova S, Celenza J, Benkovà E (2008) Auxin acts as a local morphogenetic trigger to specify lateral root founder cells. Proc Nat Acad Sci USA 105:8790–8794

Genin S (2010) Research review: molecular traits controlling host range and adaptation to plants in *Ralstonia solanacearum*. New Phytol 187:920–928

Gonzalez ET, Allen C (2003) Characterization of a *Ralstonia solanacearum* operon required for polygalacturonate degradation and uptake of galacturonic acid. Mol Plant Microbe Interact 16:536–544

Hayward AC (1991) Biology and epidemiology of bacterial wilt caused by *Pseudomonas Solanacearum*. Annu Rev Phytopathol 29:65–87

Hernandez-Blanco C, Feng DX, Hu J, Sanchez-Vallet A, Deslandes L, Llorente F, Berrocal-Lobo M, Keller H, Barlet X, Sanchez-Rodriguez C, Anderson LK, Somerville S, Marco Y, Molina A (2007) Impairment of cellulose synthases required for arabidopsis secondary cell wall formation enhances disease resistance. Plant Cell 19:890–903

Hu J, Barlet X, Deslandes L, Hirsch J, Feng DX, Somssich I, Marco Y (2008) Transcriptional responses of *Arabidopsis thaliana* during

wilt disease caused by the soil-borne phytopathogenic bacterium, *Ralstonia solanacearum*. PLoS One 3:e2589

Huang Q, Allen C (1997) An exo-poly-alpha-D-galacturonosidase, PehB, is required for wild-type virulence of *Ralstonia solanacearum*. J Bacteriol 179:7369–7378

Huckelhoven R (2007) Cell wall-associated mechanisms of disease resistance and susceptibility. Annu Rev Phytopathol 45:101–127

Liu H, Zhang S, Schell MA, Denny TP (2005) Pyramiding unmarked deletions in *Ralstonia solanacearum* shows that secreted proteins in addition to plant cell-wall-degrading enzymes contribute to virulence. Mol Plant Microbe Interact 18:1296–1305

Murashige T, Skoog F (1962) A revised medium for rapid growth and bioessays with tobacco tissue cultures. Physiol Plant 15:473–497

Nakaho K, Hibino H, Miyagawa H (2000) Possible mechanisms limiting movement of *Ralstonia solanacearum* in resistant tomato tissues. J Phytopathol 148:181–190

Oeser B, Heidrich PM, Müller U, Tudzynski P, Tenberge KB (2002) Polygalacturonase is a pathogenicity factor in the *Claviceps purpurea*/rye interaction. Fungal Genet Biol 36:176–186

Osorio S, Castillejo C, Quesada MA, Medina-Escobar N, Brownsey GJ, Suau R, Heredia A, Botella MA, Valpuesta V (2008) Partial demethylation of oligogalacturonides by pectin methyl esterase 1 is required for eliciting defence responses in wild strawberry (*Fragaria vesca*). Plant J 54:43–55

Parizot B, Laplaze L, Ricaud L, Boucheron-Dubuisson E, Bayle V, Bonke M, De Smet I, Poethig SR, Helariutta Y, Haseloff J, Chriqui D, Beeckman T, Nussaume L (2008) Diarch symmetry of the vascular bundle in Arabidopsis root encompasses the pericycle and is reflected in distich lateral root initiation. Plant Physiol 146:140–148

Pattathil S, Avci U, Baldwin D, Swennes AG, McGill JA, Popper Z, Bootten T, Albert A, Davis RH, Chennareddy C, Dong R, O'Shea B, Rossi R, Leoff C, Freshour G, Narra R, O'Neil M, York WS, Hahn MG (2010) A comprehensive toolkit of plant cell wall glycan-directed monoclonal antibodies. Plant Physiol 153:514–525

Plener L, Manfredi P, Valls M, Genin S (2010) PrhG, a transcriptional regulator responding to growth conditions, is involved in the control of the type III secretion system regulon in *Ralstonia solanacearum*. J Bacteriol 192:1011–1019

Poueymiro M, Genin S (2009) Secreted proteins from *Ralstonia solanacearum*: a hundred tricks to kill a plant. Curr Opin Microbiol 12:44–52

Saile E, McGarvey JA, Schell MA, Denny TP (1997) Role of extracellular polysaccharide and endoglucanase in root invasion and colonization of tomato plants by *Ralstonia solanacearum*. Phytopathology 87:1264–1271

Schacht T, Unger C, Pich A, Wydra K (2011) Endo- and exopolygalacturonases of *Ralstonia solanacearum* are inhibited by polygalacturonase-inhibiting protein (PGIP) activity in tomato stem extracts. Plant Physiol Biochem 49:377–387

Schell MA, Roberts DP, Denny TP (1988) Analysis of the *Pseudomonas solanacearum* polygalacturonase encoded by pglA and its involvement in phytopathogenicity. J Bacteriol 170:4501–4508

Scheller HV, Ulvskov P (2010) Hemicelluloses. Annu Rev Plant Biol 61:263–289

Tans-Kersten J, Guan Y, Allen C (1998) *Ralstonia solanacearum* pectin methylesterase is required for growth on methylated pectin but not for bacterial wilt virulence. Appl Environ Microbiol 64:4918–4923

Tasset C, Bernoux M, Jauneau A, Pouzet C, Brière C, Kieffer-Jacquinod S, Rivas S, Marco Y, Deslandes L (2010) Autoacetylation of the *Ralstonia solanacearum* effector PopP2 targets a lysine residue essential for RRS1-R-mediated immunity in Arabidopsis. PLoS Pathog 6:e1001202

Thiery J (1967) Mise en évidence des polysaccharides sur coupes fines en microscopie électronique. J Microscopie 6:987–1018

Turner M, Jauneau A, Genin S, Tavella MJ, Vailleau F, Gentzbittel L, Jardinaud MF (2009) Dissection of bacterial wilt on *Medicago truncatula* revealed two type III secretion system effectors acting on root infection process and disease development. Plant Physiol 150:1713–1722

Vailleau F, Sartorel E, Jardinaud MF, Chardon F, Genin S, Huguet T, Gentzbittel L, Petitprez M (2007) Characterization of the interaction between the bacterial wilt pathogen *Ralstonia solanacearum* and the model legume plant *Medicago truncatula*. Mol Plant Microbe Interact 20:159–167

Valette-Collet O, As Cimerman, Reignault P, Levis C, Boccara M (2003) Disruption of *Botrytis cinerea* pectin methylesterase gene *Bcpme1* reduces virulence on several host plants. Mol Plant Microbe Interact 16:360–367

Vallenet D, Labarre L, Rouy Z, Barbe V, Bocs S, Cruveiller S, Lajus A, Pascal G, Scarpelli C, Médigue C (2006) MaGe: a microbial genome annotation system supported by synteny results. Nucleic Acids Res 34:53–65

Vasse J, Frey P, Trigalet A (1995) Microscopic studies of intercellular infection and protoxylem invasion of tomato roots by *Pseudomonas solanacearum*. Mol Plant Microbe Interact 8:241–251

Vasse J, Genin S, Frey P, Boucher C, Brito B (2000) The *hrpB* and *hrpG* regulatory genes of *Ralstonia solanacearum* are required for different stages of the tomato root infection process. Mol Plant Microbe Interact 13:259–267

Vogel J, Somerville S (2000) Isolation and characterization of powdery mildew-resistant Arabidopsis mutants. Proc Natl Acad Sci USA 97:1897–1902

Vogel JP, Raab TK, Schiff C, Somerville SC (2002) *PMR6*, a pectate lyase-like gene required for powdery mildew susceptibility in Arabidopsis. Plant Cell 14:2095–2106

Vogel JP, Raab TK, Somerville CR, Somerville SC (2004) Mutations in *PMR5* result in powdery mildew resistance and altered cell wall composition. Plant J 40:968–978

Wydra K, Beri H (2006) Structural changes of homogalacturonan, rhamnogalacturonan I and arabinogalactan protein in xylem cell walls of tomato genotypes in reaction to *Ralstonia solanacearum*. Physiol Mol Plant Pathol 68:41–50

Wydra K, Beri H (2007) Immunohistochemical changes in methylester distribution of homogalacturonan and side chain composition of rhamnogalacturonan I as possible components of basal resistance in tomato inoculated with *Ralstonia solanacearum*. Physiol Mol Plant Pathol 70:13–24

Zhu Y, Nam J, Carpita NC, Matthysse AG, Gelvin SB (2003a) Agrobacterium-mediated root transformation is inhibited by mutation of an Arabidopsis cellulose synthase-like gene. Plant Physiol 133:1000–1010

Zhu Y, Nam J, Humara JM, Mysore KS, Lee LY, Cao H, Valentine L, Li J, Kaiser AD, Kopecky AL, Hwang HH, Bhattacharjee S, Rao PK, Tzfira T, Rajagopal J, Yi H, Veena, Yadav BS, Crane YM, Lin K, Larcher Y, Gelvin MJ, Knue M, Ramos C, Zhao X, Davis SJ, Kim SI, Ranjith-Kumar CT, Choi YJ, Hallan VK, Chattopadhyay S, Sui X, Ziemienowicz A, Matthysse AG, Citovsky V, Hohn B, Gelvin SB (2003b) Identification of Arabidopsis *rat* mutants. Plant Physiol 132:494–505

Zolobowska L, Van Gijsegem F (2006) Induction of lateral root structure formation on petunia roots: a novel effect of GMI1000 *Ralstonia solanacearum* infection impaired in Hrp mutants. Mol Plant Microbe Interact 19:597–606